

EXCITATION SPECTRA OF CUBIC PEROVSKITE TITANATES

LE HONG PHUC^{1,2}, NGUYEN QUAN HIEN¹,
HIEU T. NGUYEN-TRUONG^{3,†} AND HUNG M. LE⁴

¹*Ho Chi Minh City Institute of Physics, Vietnam Academy of Science and Technology,
01 Mac Dinh Chi St, Dist 01 Ho Chi Minh City, Vietnam*

²*Graduate University of Science and Technology, Vietnam Academy of Science and Technology,
18 Hoang Quoc Viet, Cau Giay, Hanoi, Vietnam*

³*Advanced Institute of Materials Science, Ton Duc Thang University, Ho Chi Minh City, Vietnam*

⁴*Department of Chemistry, Washington State University,
Pullman, Washington 99164, United States*

E-mail: †nguyentruongthanhhieu@tdtu.edu.vn

Received 4 August 2021; Accepted for publication 19 September 2021; Published 5 January 2022

Abstract. *We calculate excitation spectra of cubic perovskites $ATiO_3$ ($A = Ca, Sr, Ba, Pb$). The calculations are performed within the time-dependent density functional theory, including local field effects. The theoretical calculations show that the perovskites have a plasmon mode at around 12 eV, which is not observed in experiments.*

Keywords: perovskite; excitation spectra; dielectric function; time-dependent density functional theory.

Classification numbers: 31.15.E; 77.22.Ch.

I. INTRODUCTION

In the $ATiO_3$ -type perovskite family, barium titanate ($BaTiO_3$, BTO), strontium titanate ($SrTiO_3$, STO), calcium titanate ($CaTiO_3$, CTO), and lead titanate ($PbTiO_3$, PTO) have attracted much attention due to their potential applications in ferroelectrics and optoelectronics [1–4]. It is therefore important to understand dielectric properties of these materials. Their dielectric functions have been determined from reflectivity measurements [5–7] and calculated using the density functional theory [8–16]. The optical spectra is determined by the dielectric function. In fact, the reflectance and absorbance spectra of CTO, STO, BTO, and PTO have been extensively studied.

The previous studies have shown that low-energy absorption peaks are mainly related to interband transitions from O-2*p* valence bands to Ti-3*d* conduction bands, while high-energy ones are associated with plasmon excitation. In addition, there are discrepancies between optical absorption spectra from theoretical calculations and experimental measurements.

The perovskites have different structures. It has been shown that the optical spectra of BTO in the tetragonal and cubic phases are quite similar due to the small c/a ratio between the lattice constants. Therefore, the cubic structure is preferred to study optical properties of perovskites to simplify theoretical calculations. The perovskite ATiO₃ in the cubic phase has the space group Pm $\bar{3}$ m, with A atoms at the corners, Ti atom at the body center, and O atoms at the face centers (Fig. 1).

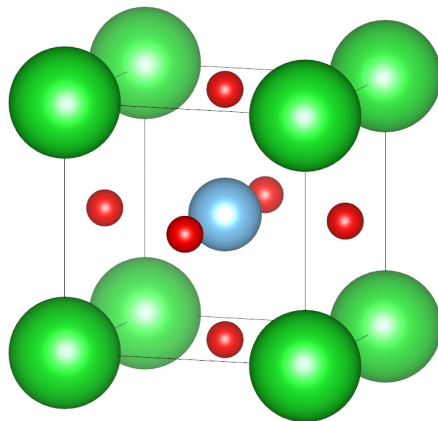


Fig. 1. (Color online) The cubic perovskites ATiO₃ with A atoms (green color) at the corners, Ti atom (blue color) at the body center, and O atoms (red color) at the face centers.

Here, we are interested in excitation spectra of cubic perovskites ATiO₃ ($A = \text{Ca, Sr, Ba, Pb}$). The excitation spectrum is given by the energy-loss function (ELF), i.e. the imaginary part of the inverse dielectric function. We calculate the ELF using the time-dependent density functional theory (TDDFT) in the random phase approximation (RPA) and adiabatic local density approximation (ALDA). Recently, we have successfully applied the TDDFT method to study excitation spectra for bulk metals [17] and two-dimensional materials [18]. The rest of paper is organized as follows: the calculation details are described in Sec. II; the results and discussion are presented in Sec. III; finally, the conclusions are given in Sec. IV.

II. COMPUTATION

The ELF is calculated using the linear response TDDFT method as implemented in the EXCITING code [19]. The ELF is given by the imaginary part of the inverse dielectric function $\epsilon(\mathbf{k}, \omega)$, i.e. $\text{Im}[-1/\epsilon(\mathbf{k}, \omega)]$. This quantity represents the probability that an electron loses energy ω and transfers momentum \mathbf{k} per unit path length traveled in the medium. Note that the Hartree atomic units ($\hbar = m_e = e = 1$) are used here. The inverse dielectric matrix is given by $\epsilon^{-1} = 1 + v\chi$, where χ is the reducible polarizability, and v is the bare Coulomb kernel. The reducible

polarizability χ is obtained by solving the Dyson equation: $\chi = \chi_0 + \chi_0(v + f_{xc})\chi$, where χ_0 is the Kohn-Sham independent-particle polarizability, and f_{xc} is the exchange-correlation kernel. Here, the RPA and ALDA kernels are used *without* and *with* local-field effects (LFE).

The ground state calculation is performed using the Perdew–Burke–Ernzerhof exchange-correlation functional and a \mathbf{k} -point grid of $30 \times 30 \times 30$. The cubic lattice constant is 3.89, 3.91, 4.04, and 3.96 Å for CTO, STO, BTO, and PTO, respectively. These values are obtained from the optimization process with input from experiments [11, 20–22]. The muffin-tin radius R_{MT}^{O} of O atoms in CTO, STO, BTO, and PTO is 1.6, 1.6, 1.8, and 1.7 Bohr, respectively; the R_{MT}^{O} of Ca, Sr, Ba, Pb, and Ti atoms are 2.0 Bohr; the product $R_{\text{min}}^{\text{MT}}|\mathbf{G} + \mathbf{k}|_{\text{max}}$ is set to 9 for CTO, STO, and BTO; to 8 for PTO. The TDDFT calculation is carried out using 100 empty states and a \mathbf{k} -point grid of $20 \times 20 \times 20$. The product $R_{\text{min}}^{\text{MT}}|\mathbf{G} + \mathbf{k}|_{\text{max}}$ is set to 7.

III. RESULTS AND DISCUSSION

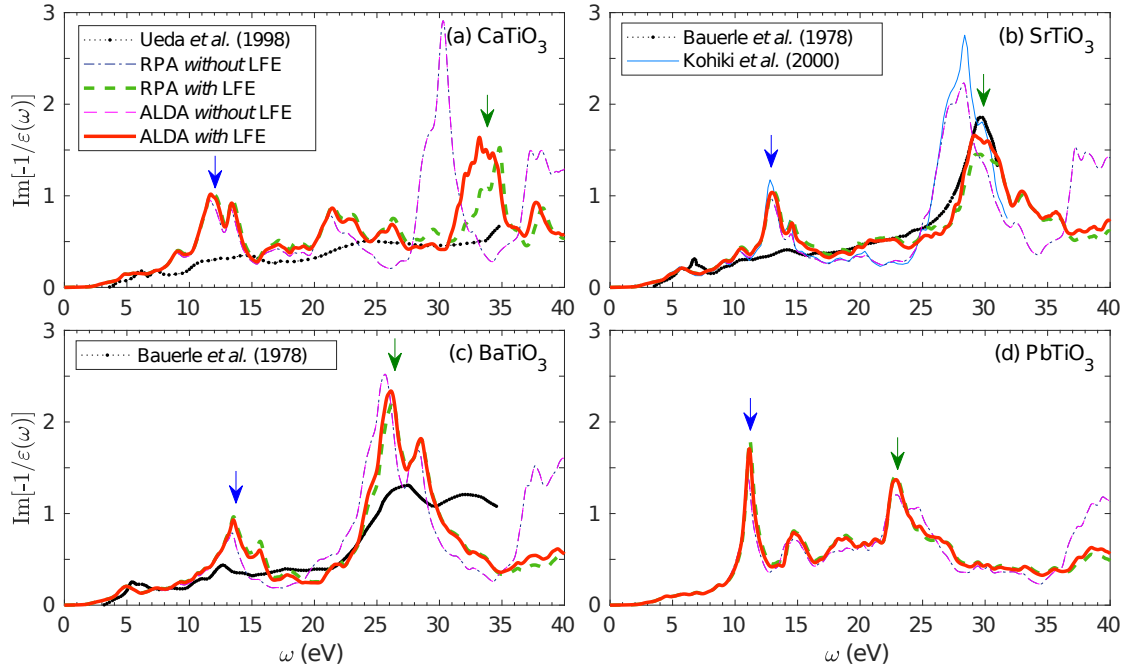


Fig. 2. (Color online) The ELF of cubic perovskite titanates: (a) CaTiO_3 , (b) SrTiO_3 , (c) BaTiO_3 , and (d) PbTiO_3 . The black dotted line is the experimental data [6, 7]. The blue line is the previous theoretical result [8]. The other lines are the present results.

Figure 2 shows the ELFs of cubic perovskite titanates. The previous theoretical results [8] (blue line) and available experimental data [6, 7] (black dotted line) are also included for comparison. The theoretical results are calculated by the full potential linearized augmented plane wave method. The experimental data are obtained from reflectivity measurements by the Kramer–Krönig transformation. Note that the perovskite structure in the measurements may not be cubic. For example, in the cases of STO and BTO, the reflectivity measurements [6] are performed at

room temperature. The structure of STO and BTO at room temperature are cubic and tetragonal, respectively. Therefore, the comparison between theoretical and experimental results is only relative.

There are differences between theoretical and experimental results. For instance, the theoretical spectra show that the perovskites have a plasmon peak in the energy range 10-15 eV, but there is no such a peak in the experimental ones. Nonetheless, the theoretical and experimental results for STO and BTO agree in the plasmon peak at energies between 25 and 30 eV.

The difference between theoretical results *without* and *with* LFE is negligible at low energies, but becomes significant as energy increases. The results *with* LFE agree better with the experimental data than those *without* LFE. These effects arise from inhomogeneity of the electron density distribution in local fields [23], and play an important role in describing optical spectra, particularly at high energies [24].

The theoretical results show that the perovskites have two plasmon modes indicated by blue and green arrows. The low-energy plasmon mode is related to the excitation of outer-shell electrons, the plasmon position is around 12 eV. Thus, the number of outer-shell electrons involved in the low-energy plasmon mode is almost the same for different perovskites. Meanwhile, the high-energy plasmon peak is associated with the excitation both inner- and outer-shell electrons, the plasmon position is redshifted with increasing the atomic number of A atoms. Thus, the number of inner-shell electrons involved in the high-energy plasmon mode is different for different perovskites.

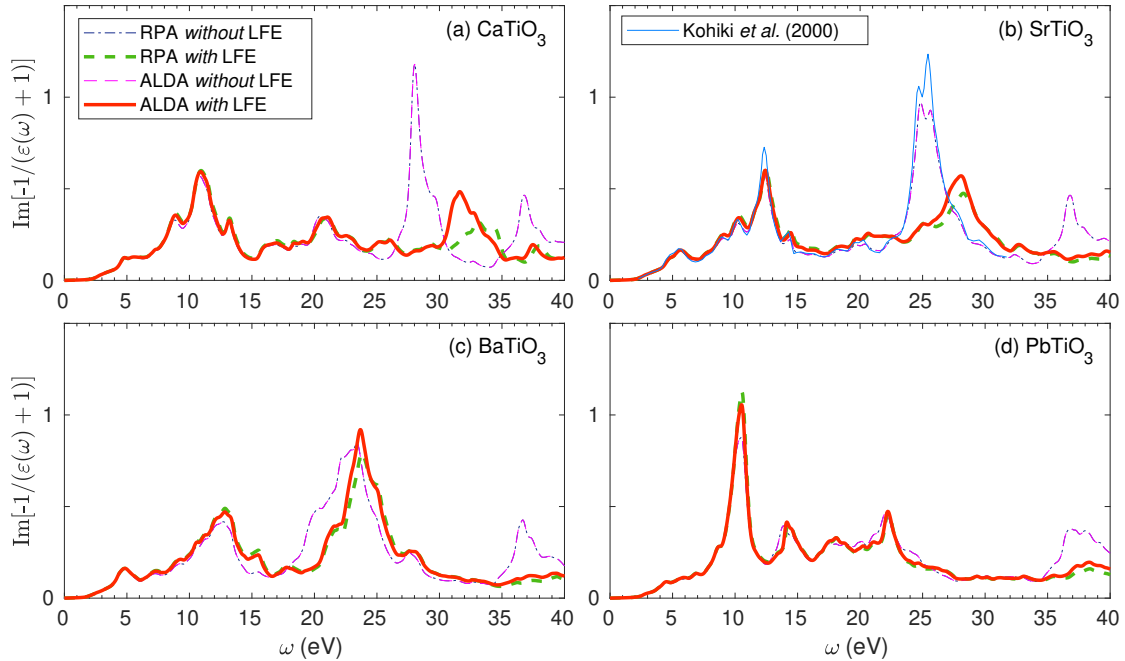


Fig. 3. The surface ELF of cubic perovskite titanates: (a) CaTiO_3 , (b) SrTiO_3 , (c) BaTiO_3 , and (d) PbTiO_3 . The blue line is the previous theoretical result [8]. The other lines are the present results.

Apart from the ELF $\text{Im}[-1/\epsilon]$, which is in fact the bulk ELF, the surface ELF $\text{Im}[-1/(\epsilon + 1)]$ is also studied. Fig. 3 shows the surface ELFs of cubic perovskite titanates. Comparing to the bulk ELF, the surface one tends to redshift slightly. A possible reason is that the number of electrons involved in the plasmon excitation at the surface is generally smaller than that in the bulk. Also, the peak intensity of the surface ELF is much lower than that of the bulk one. Thus, the excitation occurs mainly in the bulk rather than at the surface.

IV. CONCLUSIONS

We have studied excitation spectra of cubic perovskites ATiO_3 ($A = \text{Ca}, \text{Sr}, \text{Ba}, \text{Pb}$). The theoretical calculations show that the perovskites have a plasmon mode at around 12 eV, which is not observed in experiments.

ACKNOWLEDGMENT

This research is funded by Vietnam National Foundation for Science and Technology Development (NAFOSTED) under grant number 103.01-2018.300.

REFERENCES

- [1] J. Hao, W. Si, X. X. Xi, R. Guo, A. S. Bhalla and L. E. Cross, *Dielectric properties of pulsed-laser-deposited calcium titanate thin films*, *Appl. Phys. Lett.* **76** (2000) 3100.
- [2] E. Chernova, O. Pacherova, D. Chvostova, A. Dejneka, T. Kocourek, M. Jelinek and M. Tyunina, *Strain-controlled optical absorption in epitaxial ferroelectric BaTiO_3 films*, *Appl. Phys. Lett.* **106** (2015) 192903.
- [3] A. Dejneka, D. Chvostova, O. Pacherova, T. Kocourek, M. Jelinek and M. Tyunina, *Optical effects induced by epitaxial tension in lead titanate*, *Appl. Phys. Lett.* **112** (2018) 031111.
- [4] M. Tyunina, N. Nepomniashchaia, V. Vetokhina and A. Dejneka, *Optics of epitaxial strained strontium titanate films*, *Appl. Phys. Lett.* **117** (2020) 082901.
- [5] M. Cardona, *Optical Properties and Band Structure of SrTiO_3 and BaTiO_3* *Phys. Rev.* **140** (1965) A651.
- [6] D. Bäuerle, W. Braun, V. Saile, G. Sprüssel and E. E. Koch, *Vacuum ultraviolet reflectivity and band structure of SrTiO_3 and BaTiO_3* , *Zeitschrift für Phys. B Condens. Matter* **29** (1978) 179.
- [7] K. Ueda, H. Yanagi, R. Noshiro, H. Hosono and H. Kawazoe, *Vacuum ultraviolet reflectance and electron energy loss spectra of CaTiO_3* *J. Phys. Condens. Matter* **10** (1998) 3669.
- [8] S. Kohiki, M. Arai, H. Yoshikawa, S. Fukushima, M. Oku and Y. Waseda, *Energy-loss structure in core-level photoemission satellites of SrTiO_3 , $\text{SrTiO}_3:\text{La}$, and $\text{SrTiO}_3:\text{Nb}$* , *Phys. Rev. B* **62** (2000) 7964.
- [9] S. Saha, T. P. Sinha and A. Mookerjee, *Electronic structure, chemical bonding, and optical properties of paraelectric BaTiO_3* , *Phys. Rev. B* **62** (2000) 8828.
- [10] Y.-x. Wang, W.-l. Zhong, C.-l. Wang and P.-l. Zhang, *First principles study on the optical properties of cubic CaTiO_3* , *Phys. Lett. A* **291** (2001) 338.
- [11] M. Arai, S. Kohiki, H. Yoshikawa, S. Fukushima, Y. Waseda and M. Oku, *Photoelectron energy-loss functions of SrTiO_3 , BaTiO_3 , and TiO_2 : theory and experiment*, *Phys. Rev. B* **65** (2002) 085101.
- [12] M.-Q. Cai, Z. Yin and M.-S. Zhang, *First-principles study of optical properties of barium titanate*, *Appl. Phys. Lett.* **83** (2003) 2805.
- [13] G. Gupta, T. Nautiyal and S. Auluck, *Optical properties of the compounds BaTiO_3 and SrTiO_3* *Phys. Rev. B* **69** (2004) 052101.
- [14] S.-D. Guo and B.-G. Liu, *Electronic structures and optical dielectric functions of room temperature phases of SrTiO_3 and BaTiO_3* , *J. Appl. Phys.* **110** (2011) 073525.
- [15] S. Sanna, C. Thierfelder, S. Wippermann, T. P. Sinha and W. G. Schmidt, *Barium titanate ground- and excited-state properties from first-principles calculations*, *Phys. Rev. B* **83** (2011) 054112.
- [16] S. M. Hosseini, T. Movlarooy and A. Kompany, *First-principles study of the optical properties of PbTiO_3* , *Eur. Phys. J. B - Condens. Matter Complex Syst.* **46** (2005) 463.

- [17] H. T. Nguyen-Truong, *Low-energy electron inelastic mean free path in materials*, *Appl. Phys. Lett.* **108** (2016) 172901.
- [18] H. T. Nguyen-Truong, B. Da, L. Yang, Z. Ding, H. Yoshikawa and S. Tanuma, *Low-energy electron inelastic mean free path for monolayer graphene*, *Appl. Phys. Lett.* **117** (2020) 033103.
- [19] A. Gulans, S. Kontur, C. Meisenbichler, D. Nabok, P. Pavone, S. Rigamonti, S. Sagmeister, U. Werner and C. Draxl, *Exciting: a full-potential all-electron package implementing density-functional theory and many-body perturbation theory*, *J. Phys. Condens. Matter* **26** (2014) 363202.
- [20] S. Tinte, M. G. Stachiotti, C. O. Rodriguez, D. L. Novikov and N. E. Christensen, *Applications of the generalized gradient approximation to ferroelectric perovskites*, *Phys. Rev. B* **58** (1998) 11959.
- [21] B. J. Kennedy, C. J. Howard and B. C. Chakoumakos, *Phase transitions in perovskite at elevated temperatures - a powder neutron diffraction study*, *J. Phys. Condens. Matter* **11** (1999) 1479.
- [22] Y. Kuroiwa, S. Aoyagi, A. Sawada, J. Harada, E. Nishibori, M. Takata and M. Sakata, *Evidence for Pb-O Covallency in Tetragonal PbTiO₃*, *Phys. Rev. Lett.* **87** (2001) 217601.
- [23] M. Gatti, I. V. Tokatly and A. Rubio, *Sodium: a charge-transfer insulator at high pressures*, *Phys. Rev. Lett.* **104** (2010) 216404.
- [24] N. Vast, L. Reining, V. Olevano, P. Schattschneider and B. Jouffrey, *Local Field Effects in the Electron Energy Loss Spectra of Rutile TiO₂*, *Phys. Rev. Lett.* **88** (2002) 037601.